Efficient Preparation of Large-Area Graphene Oxide Sheets for Transparent Conductive Films

Jinping Zhao, Songfeng Pei, Wencai Ren,* Libo Gao, and Hui-Ming Cheng*

Shenyang National Laboratory for Materials Science, Institute of Metal Research, Chinese Academy of Sciences, Shenyang 110016, P.R. China

ABSTRACT Large-area sheets are highly desirable for fundamental research and technological applications of graphene. Here we introduce a modified chemical exfoliation technique to prepare large-area graphene oxide (GO) sheets. The maximum area of the GO sheets obtained can reach ~40000 μm^2. We found that the GO area is strongly correlated with the C—O content of the graphite oxide, which enables the area of the synthesized GO sheets to be controlled. By simply changing oxidation conditions, GO sheets with an average area of *ca.* 100—300, *ca.* 1000—3000, and ~7000 μm^2 were selectively synthesized. For transparent conductive film applications, thin GO films were fabricated by self-assembly on a liquid/air interface and reduced by HI acid. We found that the sheet resistance of the reduced GO (rGO) films decreases with increasing sheet area at the same transmittance because of the decrease in the number of intersheet tunneling barriers. The rGO film made from GO sheets with an average area of ~7000 μm^2 shows a sheet resistance of 840 Ω/sq at 78% transmittance, which is much lower than that (19.1 kΩ/sq at 79% transmittance) of a rGO film made from small-area GO sheets of *ca.* 100—300 μm^2, and comparable to that of graphene films grown on Ni by chemical vapor deposition.

KEYWORDS: graphene · large area · size control · reduction · transparent conductive film

Transparent conductive films (TCFs) have a wide range of important technological applications, such as flat displays, solar cells, optical communication devices, and solid-state lighting.[1] Graphene is widely considered to be an ideal material for the use as TCFs because of its unique two-dimensional structure, remarkable electrical conductivity, and optical transparency to visible and near-infrared light (380—1300 nm) as well as excellent mechanical properties.[2—7] In particular, large-area graphene sheets are highly desirable for TCF applications. Currently, mechanical cleavage of graphite is able to make high quality graphene reaching a millimeter size but with a very low yield.[4] Emtsev *et al*. demonstrated that graphitization of Si-terminated SiC (0001) in an argon atmosphere can produce monolayer graphene films with a large domain size of several tens of micrometers.[8] However, as well as the low yield, the graphene obtained is difficult to transfer to other substrates. Chemical vapor deposition (CVD) has recently been developed and extensively explored to grow large-area graphene by using Ni films and Cu foils, which greatly expands the applications of graphene as TCFs.[9—14]

Alternatively, chemical exfoliation starting from the oxidation of graphite is an efficient process to produce graphene on a large scale and at low cost, combined with post-reduction processes.[15—21] Moreover, the product of the chemical exfoliation of graphite oxide, that is, graphene oxide (GO), possesses different properties from graphene due to the covalent functionalization by oxygen-containing groups.[19—21] GO sheets are strongly hydrophilic and can generate stable and homogeneous colloidal suspensions in aqueous and various polar organic solvents due to the electrostatic repulsion between the negatively charged GO sheets, which makes them easy to process.[19—21] In addition, the electrical insulating property of GO sheets, owing to the disruption of graphitic networks, can be tuned and partially recovered to produce electrically conducting material (reduced GO, rGO),[16—26] by chemical reduction,[16,17,22—24] thermal annealing,[18,25] and ultraviolet excitation.[26] More importantly, compared to the porous and fragile property of graphene flake films, GO films are dense, stiff, and strong because the functional groups bind individual sheets together.[4,6] Because of the above advantages, GO sheets have been demonstrated to generate flexible TCFs with excellent mechanical properties[20] by using well-established methods, such as vacuum filtration,[27] spin-coating,[25,28] and the Langmuir—Blodgett film technique,[29,30] for the building blocks of organic electronics and solar cells.[31,32]

*Address correspondence to cheng@imr.ac.cn, wcren@imr.ac.cn.

Received for review July 7, 2010 and accepted August 27, 2010.

Published online September 3, 2010. 10.1021/nn1015506

However, the GO sheets currently used for the fabrication of TCFs are small,[25,27,31−34] mostly with an area in the order of 100 μm^2, because of the difficulty in the production of large-area GO sheets, i.e., unavoidable breaking of GO sheets during the vigorous oxidation and exfoliation processes. The small area of GO sheets results in high intersheet contact resistance in their rGO films due to a large amount of intersheet junctions.[20] Very recently, two groups reported the synthesis of ultralarge GO sheets by modifying the oxidation/exfoliation in the Hummers' method.[35,36] However, Su *et al.* found that the ultralarge GO sheets break into small domains after high-temperature reduction.[35] In addition, the sp^2 conjugated carbon network in GO sheets is only partially recovered by the present reduction methods,[20] and this hinders efficient charge transport through the atomically thin plane. As a result, the reported properties of TCFs made from GO sheets are significantly lower than those of TCFs made from CVD-grown graphene. Therefore, both synthesis and efficient and nondestructive reduction of large-area GO sheets are essentially important for improving the properties of GO-based TCFs.

We demonstrate the synthesis of large GO sheets by a modified chemical exfoliation method. The largest graphene sheet can reach ~40000 μm^2 in area. Moreover, we found that the area of GO sheets is strongly correlated to the C−O content of graphite oxide, and that this can be controlled, to a certain extent, by simply changing the oxidation conditions. For TCF applications, the GO films were fabricated using a self-assembly method on a liquid/air interface[37] and reduced by HI acid, an efficient reduction method recently developed by our group.[38] We found that the sheet electrical resistance of the rGO films decreases with increasing area of GO sheets at the same transmittance because of the decrease in the number of intersheet tunneling barriers. The electrical resistivity of the TCF made from large GO sheets of ~7000 μm^2 in area is ~840 Ω/sq at 78% transmittance, which is ~20 times lower than that (19.1 kΩ/sq at 79% transmittance) of TCF made from the small GO sheets of *ca.* 100−300 μm^2 in area, and comparable to that of CVD-grown graphene on Ni.

RESULTS AND DISCUSSION

Preparation and Reduction of Large-Area GO Sheets. Generally, the preparation of GO sheets by chemical exfoliation consists of three key steps: the oxidation of graphite to obtain graphite oxide, the exfoliation of graphite oxide to prepare GO sheets by sonication, subsequent dispersion, and centrifugation to remove thick graphite flakes. To prepare large-area GO sheets, three modifications were made in our experiments: (1) using graphite with a large lateral size (nature flake graphite with an average size of 500−600 μm) as starting material to prepare large-area graphite oxide; (2) applying mild oxidation and sonication to avoid the overcracking of graphite during oxidation and exfoliation; (3) using a two-step centrifugation to successively remove thick multilayer flakes and small flakes.

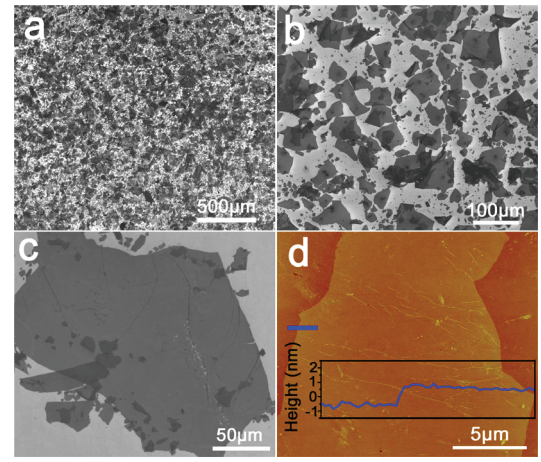

Figure 1. (a−c) SEM and (d) AFM images of large-area GO sheets. The inset of panel d shows that the thickness of the measured GO sheets is ~1.2 nm.

Figure 1 shows typical scanning electron microscopy (SEM) and atomic force microscopy (AFM) images of GO sheets obtained by the modified chemical exfoliation. It is worth noting that most of the GO sheets are about 10000 μm^2 in area (Figure 1a,b), which is much larger than those reported previously,[16,17,29,39−41] usually having a lateral size in the range of hundreds of nanometers to a few micrometers, and similar to those reported very recently.[35,36] The largest GO sheet observed can reach ~40000 μm^2 (Figure 1c). Because of van der Waals interactions between GO sheets, some GO sheets were overlapped on the substrate after pulling the substrate out of the GO suspension, as shown in Figure 1a,b. Because of the presence of covalently bonded oxygen and the displacement of sp^3-hybridized carbon atoms slightly above and below the original graphene plane, the monolayer GO sheets are much thicker than monolayer graphene, with a thickness of ~1.0 nm.[16] A large number of AFM measurements shows that most of the GO sheets obtained are 0.8−1.2 nm in thickness, as shown in Figure 1d, indicating that these GO sheets are monolayer.

The presence of oxygen-containing groups on a graphene plane disrupts the sp^2 bonding nature of carbon atoms, resulting in the insulating nature of GO sheets. To improve the electrical conductivity of large-area GO sheets, we reduced the large-area GO sheets by HI acid.[38] Figure 2 panels a and c show typical optical images of the as-prepared individual GO sheets and those reduced by HI acid. The as-prepared GO sheets are almost transparent with a very light contrast with the substrate, which confirms the insulating nature of GO sheets. The small blue regions near the edges, corresponding to a larger thickness, are attributed to the commonly observed edge folding.[42] It is interesting to

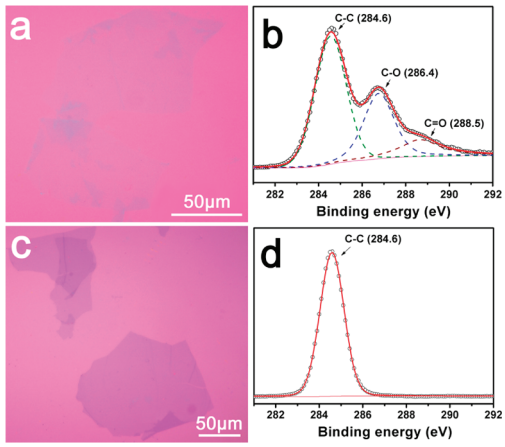

Figure 2. Typical optical images and C 1s XPS spectra of the as-prepared GO (a,b) and rGO sheets reduced by HI acid (c,d).

note that the contrast of GO sheets with the substrate is remarkably increased after HI acid reduction, indicating the effective reduction and appreciable improvement in their electrical conductivity. Moreover, no cracking and area decrease of the GO sheets were observed after HI acid reduction. This is quite different from high-temperature annealing reduction in which Su *et al*. found that ultralarge GO sheets break into small domains after treatment at 800 °C.[35]

We also performed X-ray photoelectron spectroscopy (XPS) measurements on the GO sheets before and after reduction to evaluate the removal of oxygen-containing groups by HI acid. The C1s XPS spectrum of the as-prepared GO sheets (Figure 2b) clearly shows considerable oxygen content with two components that correspond to carbon atoms in different functional groups: the carbon in C−O bonds (hydroxyl and epoxy, 286.4 eV), and the carbonyl carbon (C═O, 288.5 eV), in addition to the nonoxygenated ring carbon (C−C, 284.6 eV). After reduction, the C 1s XPS spectrum becomes a single symmetrical peak at 284.4 eV (Figure 2d), and the carbon to oxygen (C/O) ratio (~12) is much higher than that reduced by many other methods, strongly suggesting that most oxygen-containing groups are effectively removed during HI acid reduction. These results open up the possibility for synthesis of large-area rGO sheets with good electrical conductivity, which paves the way for the electrical property-related applications of large-area GO sheets.

Area-Controlled Preparation of GO Sheets and Its Mechanism. To elucidate the formation of large-area GO sheets and achieve area-controlled synthesis, we investigated the effects of oxidation parameters on the area of GO sheets obtained. Large-area GO sheets were prepared using the procedure described in the Experimental Section: Preparation of Large-Area GO Sheets, which is referred to as condition I. In condition II, a high temperature stirring at 90 °C for 2 h was used in addition to the stirring at 0 and 35 °C during oxidation, and the other

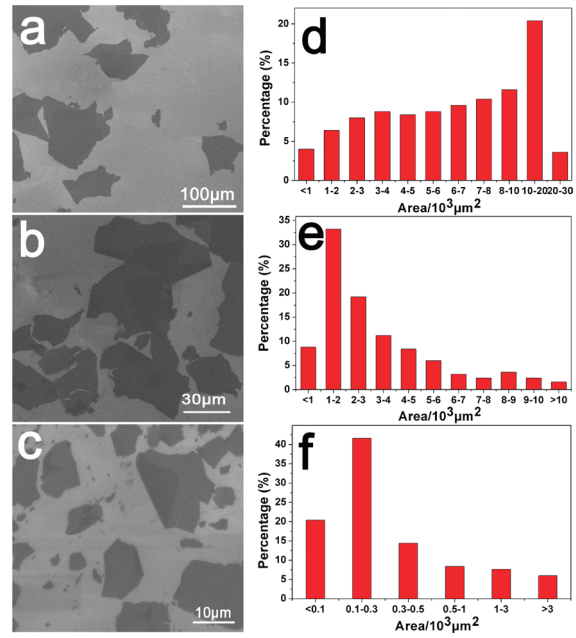

Figure 3. Typical SEM images and the corresponding area distributions of samples I (a,d), II (b,e), and III (c,f).

parameters were kept the same as those of condition I. For the third case (condition III), we doubled the $KMnO_4$ amount for the oxidation of graphite while keeping the other parameters the same as those of condition II. For the following discussion, the GO sheets prepared with conditions I, II, and III are defined as samples I, II, and III, respectively.

Figure 3 panels a, b, and c show the typical SEM images of the GO sheets obtained from the three different oxidation conditions. It is clearly seen that the area of the GO sheets changes with changing oxidation parameters. On the basis of SEM measurements on 250 sheets for each sample, we obtained the respective area distributions. In sample I, ~56% of GO sheets are larger than 7000 μm^2 (Figure 3d). When an additional high-temperature oxidation at 90 °C was used, the GO sheets (sample II) become smaller, with ~52% of them having an area of *ca.* 1000−3000 μm^2 (Figure 3e). Much smaller GO sheets are obtained if we further increase the oxidation by doubling the amount of $KMnO_4$ (sample III), and ~41% of GO sheets have an area of *ca.* 100−300 μm^2 (Figure 3f).

The C/O atomic ratio is an important parameter for evaluating the oxidation degree of graphite oxide and GO sheets. Considering the strong binding between oxygen-containing groups and the graphene plane, we believe that the oxygen content of all the GO sheets obtained remains almost the same as that of the graphite oxide used. To understand the effect of the oxidation parameters on the area of the GO sheets, we analyzed the C/O atomic ratio of the sheets in samples I, II, and III from XPS spectra. It is found that the C/O atomic ratio of the sheets decreases from 2.63 to 2.57 when an additional high temperature stirring at 90 °C was used, and

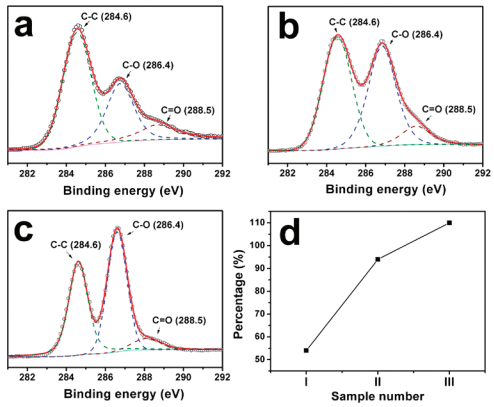

Figure 4. Typical C1s XPS spectra of GO sheets in sample I (a), II (b), and III (c), and the corresponding peak area ratio of C−O to C−C (d).

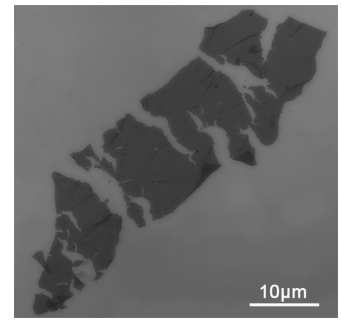

Figure 5. SEM image of several pieces of GO sheets with a high C−O content, showing that the small sheets come from the cracking of a big sheet.

further decreases to 2.08 when the amount of $KMnO_4$ was doubled. These results indicate that the oxidation degree of both the GO sheets and the graphite oxide increase with increasing oxidation temperature and concentration of oxidant.

To elucidate how the oxidation degree of graphite oxide affects the size of the GO sheets, we analyzed the C1s XPS spectra of GO sheets in samples I, II, and III. Solid-state ^{13}C NMR spectroscopy of graphite oxide and recently ^{13}C-labeled graphite oxide indicates that a significant fraction of the sp^2-bonded carbon network in graphite oxide is bonded with hydroxyl groups or epoxide groups, while minor components of carboxylic or carbonyl groups are located on graphene edges.[19,21,43] This is the reason why a much stronger C1s XPS peak is usually observed at 286.4 eV, corresponding to hydroxyl and epoxide groups, than that at 288.5 eV (corresponding to carboxylic or carbonyl groups), as shown in Figure 2c. Figure 4 shows the typical C1s XPS spectra of the GO sheets with different oxidation conditions. It is interesting to find that the peak area ratio of C−O to C−C dramatically increases from 54% for sample I to 94% for sample II and then to 110% for sample III with an increase in the oxidation degree. This indicates a great increase in the content of hydroxyl and epoxide groups grafted on the carbon network of graphene layers with enhanced oxidation.

The grafting of oxygen-containing groups on the surface of graphene layers increases the interlayer spacing of graphite oxide, which consequently decreases the van der Waals interlayer interactions and makes the layered graphite oxide easier to cleave. At the same time, the binding of oxygen-containing groups on carbon atoms changes the graphene layers from planar sp^2-hybridized to a distorted sp^3-hybridized geometry. It was reported that the oxygen atom in triangular epoxy groups (C−O−C) acts as a minuscule wedge, pushing apart the bridge carbon atoms and stretching the C−C bond.[44,45] Therefore, the formation of oxygen-containing groups severely decreases the bond energy between carbon atoms within the carbon network. Recently, Wu *et al*. found that chemically derived graphene sheets can be sonochemically cut along parallel line faults on their surface to effectively fabricate graphene nanoribbons,[46] which provides supporting evidence for the weaker interactions of stretched C−C bonds or C−O−C bonds than the normal C−C bond.[44] As a result, when ultrasonic treatment is used to separate the decoupled graphene layers in graphite oxide to form individual GO sheets, the sonochemical effects and ultrahot gas bubbles simultaneously break the stretched C−C bonds or C−O−C bonds, leading to the cracking of graphene layers. Therefore, it is reasonable to believe that the higher C−O content in graphite oxide makes layer cracking much easier due to the presence of more stretched C−C bonds or C−O−C bonds. Figure 5 shows a typical image of a GO sheet in sample III with high C−O content after mild sonication, which clearly shows the cracking of a whole GO sheet. It is worth noting that this is rarely observed for GO sheets in sample I with a low C−O content. On the basis of the above observations and analyses, we suggest that the content of C−O groups in graphite oxide plays a key role in controlling the area of the GO sheets obtained, which provides useful information on the area-controlled synthesis of GO sheets by chemical exfoliation.

TCF Properties of GO Sheets with Different Areas. We compared the properties of TCFs assembled from GO sheets with different average areas. As described above, the presence of oxygen-containing groups hinders charge transport through the atomically thin plane because of the absence of percolating pathways among sp^2 carbon clusters.[20] Efficient reduction to restore the sp^2-conjugated graphene network is the prerequisite for the use of GO as a TCF. Compared to the current low temperature chemical reduction that can only yield moderate optoelectronic properties, high temperature annealing at 1100 °C yields the highest degree of reduction and the best properties of films, with a sheet resistance of a few KΩ/sq at transmittance of 90%.[20,25] However, high temperature reduction must be avoided for GO films on low melting-point substrates, such as plastic platforms and glass, in TCF applications. Recently, we

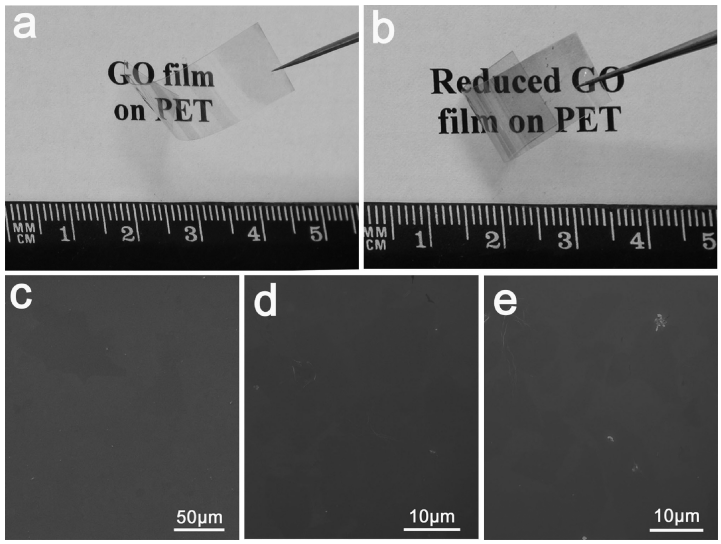

Figure 6. Optical images of GO films (a) before and (b) after HI acid reduction. Typical SEM images of the GO films after reduction assembled with (c) sample I, (d) sample II, and (e) sample III GO sheets.

developed a rapid and nondestructive low temperature approach for the highly efficient reduction of GO films by HI acid.[38] This reduction is based on the halogenation reaction of hydroxyl groups. GO films can be reduced at low temperature (≤100 °C) within a few minutes or even less than one minute for thin films. More importantly, the reduced GO films maintain the integrity and flexibility of the original GO film. In contrast, the widely used hydrazine and sodium borohydride reductions usually lead to severe expansion or break up of the GO films, which is fatal for their application as a TCF. Considering the compatibility requirement of GO sheets with glass or plastic platforms in future application as TCFs, we therefore used HI acid to reduce the assembled GO films. Figure 6 panels a and b show the optical images of GO films assembled on PET substrates before and after HI acid reduction. As with the observations on individual GO sheets (Figure 2), the GO films are almost transparent, while they change to light gray after HI acid reduction, indicating an appreciable improvement of electrical conductivity. XPS confirms the efficient removal of oxygen-containing groups, with a C/O atomic ratio of ~12 after reduction (Supporting Information). Moreover, the rGO films are doped with a low concentration of residual iodine (~0.3%), which is thermally stable[38] and favorable for the further improvement in the electrical conductivity of rGO films.[47,48]

Figures 6c−e and 7 show SEM images of rGO film-based TCFs made from GO sheets with different areas, and the corresponding sheet resistance and transmittance. It can be seen that the sheet resistance of TCFs greatly decreases with increasing GO sheet area at the same transmittance. Approximately, a one order-of-magnitude decrease in sheet resistance is achieved when the area of GO sheets increases from *ca.* 100−300 to 7000 μm^2. For example, at a transmittance of 78%, the TCF made from sample I (~7000 μm^2 in area) has a sheet resistance of ~840 Ω/sq, which is much lower than those of TCFs made from sample II (*ca.* 1000−3000 μm^2 in area, ~5.6 kΩ/sq with a transparency of 77%) and from sample III (*ca.* 100−300 μm^2 in area, ~19.1 kΩ/sq with a transparency of 79%). Considering the same reduction conditions, we believe that the higher electrical conductivity of TCFs made from sample I than those made from samples II and III is mainly due to the increase in average sheet area and consequent decrease in the number of intersheet tunneling barriers in a continuous rGO film.

Recently, De *et al.*, proposed a figure of merit, the direct current to optical conductivity ratio (σ_{DC}/σ_{OP}), to evaluate the opto-electrical properties of graphene-based films, which allows comparison with different materials including commercial indium tin oxide.[49] A high value of σ_{DC}/σ_{OP} represents the desired opto-electrical property for TCFs (high transmittance and low sheet resistance). To evaluate the properties of TCF made from large-area GO sheets, we adopted σ_{DC}/σ_{OP} as a criterion. The calculated σ_{DC}/σ_{OP} value for TCFs made from large-area GO sheets is 2.0. Table 1 in Supporting Information (Table S1) lists the calculated σ_{DC}/σ_{OP} values for TCFs made from different kinds of graphene, including rGO produced by various chemical reduction techniques, high temperature annealing, and a combination of these two methods, solution-exfoliated graphene sheets by sonication of graphite, and CVD-grown graphene. It is worth noting that the σ_{DC}/σ_{OP} of TCF made from large-area rGO sheets is much higher than those of TCFs made from other chemically reduced GO, even high temperature rGO, and solution-exfoliated graphene sheets by sonication of graphite. Considering the high quality and

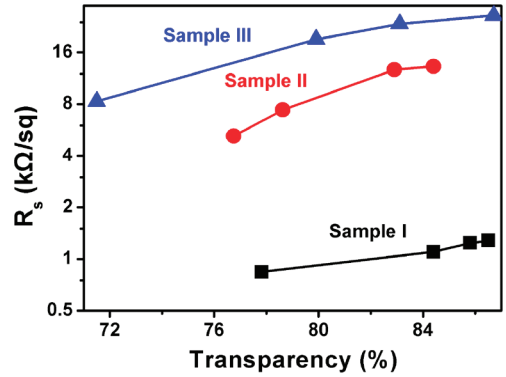

Figure 7. Sheet resistance and transmittance at 550 nm of TCFs assembled with sample I, sample II, and sample III GO sheets.

small size of liquid-exfoliated graphene, the much better performance of TCFs made from large-area GO sheets further confirms that the electrical conductivity of graphene films is mainly limited by intersheet junctions.[49] More surprisingly, this value is comparable to that of graphene films prepared by CVD on Ni (σ_{DC}/σ_{OP} of *ca.* 4−5, see Supporting Information), showing great potential for fabricating high-performance TCFs at a low cost by using large-area GO sheets and highly efficient HI acid reduction. We believe that the properties of TCFs made from GO sheets can be further improved by using larger GO sheets, improving the intersheet contact, proper doping, and developing more efficient reduction and assembly methods.

CONCLUSION

We developed a modified chemical exfoliation method to produce large-area GO sheets. By using mild oxidation, sonication, and two-step centrifugation, GO sheets with an area up to ~40000 μm^2 were obtained. Moreover, we found that the area of GO sheets obtained is strongly correlated to the C−O content in the graphite oxide, which enables the area-controlled synthesis of GO sheets. By simply changing the oxidation conditions, GO sheets with average areas of *ca.* 100−300, *ca.* 1000−3000, and ~7000 μm^2 were selectively obtained. The sheet resistance of rGO-based TCFs decreases with increasing GO sheet area with the same transmittance because of the decrease in the number of intersheet tunneling barriers. A TCF made from large-area rGO sheets by HI acid reduction shows a sheet resistance of ~840 Ω/sq at a transmittance of 78%, which is much lower than the values reported for TCFs made from chemically reduced, high temperature annealing-reduced GO sheets, and solution-exfoliated graphene sheets, and comparable to that of graphene films prepared by CVD on Ni. These findings open up the possibility for the area-controlled preparation of GO sheets, and highlight the importance of large-area GO sheets in improving the performance of rGO-based TCFs.

EXPERIMENTAL SECTION

Preparation of Large-Area GO Sheets. The detailed experimental procedure for the preparation of large-area GO sheets is described as follows. A 2 g portion of natural flake graphite with an average size of 500−600 μm, 2 g of $NaNO_3$, and 96 mL of concentrated H_2SO_4 were mixed at 0 °C. During the following stages the mixture was continuously stirred using a magnet stirrer. 12 g of $KMnO_4$ was gradually added to the above mixture while keeping the temperature at 0 °C. The mixture obtained was first stirred at 0 °C for 90 min and then at 35 °C for 2 h. Distilled water (80 mL) was slowly dropped into the resulting solution, over a period of around 30 min, to dilute the mixture. Then 200 mL of distilled water was added followed by 10 mL of H_2O_2 (30%), and the stirring continued for 10 min to obtain a graphite oxide suspension. During this final step, H_2O_2 (30%) reduced the residual permanganate and manganese dioxide to colorless soluble manganese sulfate. The graphite oxide deposit was collected from the graphite oxide suspension by high-speed centrifugation at 16000 rpm for 10 min, and repeatedly washed with distilled water until the pH = 7. Then a mild sonication (80 W, 5 min) was used to exfoliate the graphite oxide to obtain a GO suspension. To obtain uniform large-area GOs, a low-speed centrifugation at 3000 rpm was first used to remove thick multilayer flakes until all the visible particles were removed (3−5 min). Then the supernatant was further centrifuged at 5000 rpm for 5 min to separate large flakes (precipitate) and small flakes (supernatant). Finally, the obtained precipitates containing large flakes were redispersed in water to get a large-area GO sheet suspension. To determine the yield of this process, we measured the weight of the above precipitate containing large flakes after drying in a vacuum oven at 90 °C for 24 h to completely remove the water. The weight of large flakes obtained from the original 2 g of sample was about 0.25 g.

Fabrication and Reduction of GO Films for TCFs. The GO films were fabricated by a self-assembly method on a liquid/air interface as reported by Chen *et al.*[37,50] and Zhu *et al.*[33] The GO hydrosol was heated at 60 °C for a short period (from 5 to 15 min to tune the thickness of the film) in a water bath to obtain GO films on the surface of the aqueous dispersion (*i.e.*, at the air−water interface). The GO film was then collected on a PET substrate by dip coating, followed by drying at 80 °C for 3 h. To improve the electrical conductivity of the GO films for use as TCFs, they were dipped in a HI aqueous solution (55%) at 100 °C for 30 s, and then washed repeatedly with ethanol to remove the residual HI. Details about the reduction of GO films by HI acid have been reported elsewhere.[38]

Characterization of GO, rGO, and rGO Film-Based TCFs. The structure of the GO sheets was characterized by optical microscopy (Olympus Metallurgical Microscopes BX2M/MX51 with MPLFLN objective lens), SEM (FEI Nova NanoSEM 430, 15 kV), and AFM (Veeco MultiMode/NanoScope IIIa, operating in the tapping mode), and their composition was evaluated by XPS (ESCALAB 250 using focused monochromatized Al Kα radiation (1486.6 eV)). For the structural characterization, we used a dip coating method to prepare the specimen. Typically, a Si wafer capped with a 280 nm thick SiO_2 substrate was dipped into a diluted GO suspension and then slowly withdrawn from the solution at a constant speed of 0.1 mm/min, allowing for the deposition of a large amount of GO sheets on the substrate surface. GO powders were used for XPS characterization.

The structure of rGO film-based TCFs was characterized by SEM. The sheet resistance was measured by a four-probe configuration with an electrochemical workstation (Solartron1260/1287), and transmittance at a 550 nm wavelength was evaluated with a UV−vis spectrometer (Varian Cary 5000).

Acknowledgment. The authors thank Mr. Z. Wu and Z. Chen for their valuable discussions. This work was supported by National Science Foundation of China (Nos. 50872136, 50921004, and 50972147), Chinese Academy of Sciences (No. KJCX2-YW-231), and Key Laboratory of Material Corrosion and Protection of Sichuan Colleges and Universities, China (No.2008CL01).

Supporting Information Available: XPS spectra of the rGO films assembled with GO sheets with different average areas, and the calculated σ_{DC}/σ_{OP} values for TCFs made from different kinds of graphene, including rGO by chemical reduction, high temperature annealing, and a combination of these two methods; exfoliated graphene sheets by sonication of graphite, and CVD-grown graphene. This material is available free of charge *via* the Internet at http://pubs.acs.org.

REFERENCES AND NOTES

1. Cao, Q.; Rogers, J. A. Ultrathin Films of Single-Walled Carbon Nanotubes for Electronics and Sensors: A Review of Fundamental and Applied Aspects. *Adv. Mater.* **2009**, *21*, 29–53.

2. Novoselov, K. S.; Geim, A. K.; Morozov, S. V.; Jiang, D.; Zhang, Y.; Dubonos, S. V.; Grigorieva, I. V.; Firsov, A. A. Electric Field Effect in Atomically Thin Carbon Films. *Science* **2004**, *306*, 666–669.
3. Nair, R. R.; Blake, P.; Grigorenko, A. N.; Novoselov, K. S.; Booth, T. J.; Stauber, T.; Peres, N. M. R.; Geim, A. K. Fine Structure Constant Defines Visual Transparency of Graphene. *Science* **2008**, *320*, 1308.
4. Geim, A. K. Graphene: Status and Prospects. *Science* **2009**, *324*, 1530–1534.
5. Geim, A. K.; Novoselov, K. S. The Rise of Graphene. *Nat. Mater.* **2007**, *6*, 183–191.
6. Dikin, D. A.; Stankovich, S.; Zimney, E. J.; Piner, R. D.; Dommett, G. H. B.; Evmenenko, G.; Nguyen, S. T.; Ruoff, R. S. Preparation and Characterization of Graphene Oxide Paper. *Nature* **2007**, *448*, 457–460.
7. Lee, C.; Wei, X. D.; Kysar, J. W.; Hone, J. Measurement of the Elastic Properties and Intrinsic Strength of Monolayer Graphene. *Science* **2008**, *321*, 385–388.
8. Emtsev, K. V.; Bostwick, A.; Horn, K.; Jobst, J.; Kellogg, G. L.; Ley, L.; McChesney, J. L.; Ohta, T.; Reshanov, S. A.; Rohrl, J.; *et al*. Towards Wafer-Size Graphene Layers by Atmospheric Pressure Graphitization of Silicon Carbide. *Nat. Mater.* **2009**, *8*, 203–207.
9. Kim, K. S.; Zhao, Y.; Jang, H.; Lee, S. Y.; Kim, J. M.; Kim, K. S.; Ahn, J. H.; Kim, P.; Choi, J. Y.; Hong, B. H. Large-Scale Pattern Growth of Graphene Films for Stretchable Transparent Electrodes. *Nature* **2009**, *457*, 706–710.
10. Li, X. S.; Cai, W. W.; An, J. H.; Kim, S.; Nah, J.; Yang, D. X.; Piner, R.; Velamakanni, A.; Jung, I.; Tutuc, E.; *et al*. Large-Area Synthesis of High-Quality and Uniform Graphene Films on Copper Foils. *Science* **2009**, *324*, 1312–1314.
11. Reina, A.; Jia, X. T.; Ho, J.; Nezich, D.; Son, H. B.; Bulovic, V.; Dresselhaus, M. S.; Kong, J. Large Area, Few-Layer Graphene Films on Arbitrary Substrates by Chemical Vapor Deposition. *Nano Lett.* **2009**, *9*, 30–35.
12. Bae, S.; Kim, H. K.; Lee, Y. B.; Xu, X. F.; Park, J. S.; Zheng, Y.; Balakrishnan, J.; Lei, T.; Kim, H. R.; Song, Y.; *et al*. Roll-to-Roll Production of 30-Inch Graphene Films for Transparent Electrodes. *Nat. Nanotechnol.* **2010**, *5*, 574–578.
13. Li, X. S.; Zhu, Y. W.; Cai, W. W.; Borysiak, M.; Han, B. Y.; Chen, D.; Piner, R. D.; Colombo, L.; Ruoff, R. S. Transfer of Large-Area Graphene Films for High-Performance Transparent Conductive Electrodes. *Nano Lett.* **2009**, *9*, 4359–4363.
14. Chae, S. J.; Gunes, F.; Kim, K. K.; Kim, E. S.; Han, G. H.; Kim, S. M.; Shin, H. J.; Yoon, S. M.; Choi, J. Y.; Park, M. H.; *et al*. Synthesis of Large-Area Graphene Layers on Poly-Nickel Substrate by Chemical Vapor Deposition: Wrinkle Formation. *Adv. Mater.* **2009**, *21*, 2328–2333.
15. Schniepp, H. C.; Li, J. L.; McAllister, M. J.; Sai, H.; Herrera-Alonso, M.; Adamson, D. H.; Prud'homme, R. K.; Car, R.; Saville, D. A.; Aksay, I. A. Functionalized Single Graphene Sheets Derived from Splitting Graphite Oxide. *J. Phys. Chem. B* **2006**, *110*, 8535–8539.
16. Stankovich, S.; Dikin, D. A.; Piner, R. D.; Kohlhaas, K. A.; Kleinhammes, A.; Jia, Y.; Wu, Y.; Nguyen, S. T.; Ruoff, R. S. Synthesis of Graphene-Based Nanosheets *via* Chemical Reduction of Exfoliated Graphite Oxide. *Carbon* **2007**, *45*, 1558–1565.
17. Stankovich, S.; Dikin, D. A.; Dommett, G. H. B.; Kohlhaas, K. M.; Zimney, E. J.; Stach, E. A.; Piner, R. D.; Nguyen, S. T.; Ruoff, R. S. Graphene-Based Composite Materials. *Nature* **2006**, *442*, 282–286.
18. Wu, Z. S.; Ren, W. C.; Gao, L. B.; Liu, B. L.; Jiang, C. B.; Cheng, H. M. Synthesis of High-Quality Graphene with a Pre-determined Number of Layers. *Carbon* **2009**, *47*, 493–499.
19. Dreyer, D. R.; Park, S.; Bielawski, C. W.; Ruoff, R. S. The Chemistry of Graphene Oxide. *Chem. Soc. Rev.* **2010**, *39*, 228–240.
20. Eda, G.; Lin, Y. Y.; Mattevi, C.; Yamaguchi, H.; Chen, H. A.; Chen, I. S.; Chen, C. W.; Chhowalla, M. Blue Photoluminescence from Chemically Derived Graphene Oxide. *Adv. Mater.* **2010**, *22*, 505–509.
21. Park, S.; Ruoff, R. S. Chemical Methods for the Production of Graphenes. *Nat. Nanotechnol.* **2009**, *4*, 217–224.
22. Stankovich, S.; Piner, R. D.; Chen, X. Q.; Wu, N. Q.; Nguyen, S. T.; Ruoff, R. S. Stable Aqueous Dispersions of Graphitic Nanoplatelets *via* the Reduction of Exfoliated Graphite Oxide in the Presence of Poly (Sodium 4-Styrenesulfonate). *J. Mater. Chem.* **2006**, *16*, 155–158.
23. Wang, H. L.; Robinson, J. T.; Li, X. L.; Dai, H. J. Solvothermal Reduction of Chemically Exfoliated Graphene Sheets. *J. Am. Chem. Soc.* **2009**, *131*, 9910–9911.
24. Shin, H. J.; Kim, K. K.; Benayad, A.; Yoon, S. M.; Park, H. K.; Jung, I. S.; Jin, M. H.; Jeong, H. K.; Kim, J. M.; Choi, J. Y.; *et al*. Efficient Reduction of Graphite Oxide by Sodium Borohydrilde and Its Effect on Electrical Conductance. *Adv. Funct. Mater.* **2009**, *19*, 1987–1992.
25. Becerril, H. A.; Mao, J.; Liu, Z.; Stoltenberg, R. M.; Bao, Z.; Chen, Y. Evaluation of Solution-Processed Reduced Graphene Oxide Films as Transparent Conductors. *ACS Nano* **2008**, *2*, 463–470.
26. Williams, G.; Seger, B.; Kamat, P. V. TiO_2-Graphene Nanocomposites. UV-Assisted Photocatalytic Reduction of Graphene Oxide. *ACS Nano* **2008**, *2*, 1487–1491.
27. Eda, G.; Fanchini, G.; Chhowalla, M. Large-Area Ultrathin Films of Reduced Graphene Oxide as a Transparent and Flexible Electronic Material. *Nat. Nanotechnol.* **2008**, *3*, 270–274.
28. Wu, J. B.; Becerril, H. A.; Bao, Z. N.; Liu, Z. F.; Chen, Y. S.; Peumans, P. Organic Solar Cells with Solution-Processed Graphene Transparent Electrodes. *Appl. Phys. Lett.* **2008**, *92*, 263302.
29. Cote, L. J.; Kim, F.; Huang, J. X. Langmuir−Blodgett Assembly of Graphite Oxide Single Layers. *J. Am. Chem. Soc.* **2009**, *131*, 1043–1049.
30. Li, X. L.; Zhang, G. Y.; Bai, X. D.; Sun, X. M.; Wang, X. R.; Wang, E.; Dai, H. J. Highly Conducting Graphene Sheets and Langmuir−Blodgett Films. *Nat. Nanotechnol.* **2008**, *3*, 538–542.
31. Eda, G.; Lin, Y. Y.; Miller, S.; Chen, C. W.; Su, W. F.; Chhowalla, M. Transparent and Conducting Electrodes for Organic Electronics from Reduced Graphene Oxide. *Appl. Phys. Lett.* **2008**, *92*, 233305.
32. Wang, X.; Zhi, L. J.; Mullen, K. Transparent, Conductive Graphene Electrodes for Dye-Sensitized Solar Cells. *Nano Lett.* **2008**, *8*, 323–327.
33. Zhu, Y. W.; Cai, W. W.; Piner, R. D.; Velamakanni, A.; Ruoff, R. S. Transparent Self-Assembled Films of Reduced Graphene Oxide Platelets. *Appl. Phys. Lett.* **2009**, *95*, 103104.
34. Kim, Y. K.; Min, D. H. Durable Large-Area Thin Films of Graphene/Carbon Nanotube Double Layers as a Transparent Electrode. *Langmuir* **2009**, *25*, 11302–11306.
35. Su, C. Y.; Xu, Y. P.; Zhang, W. J.; Zhao, J. W.; Tang, X. H.; Tsai, C. H.; Li, L. J. Electrical and Spectroscopic Characterizations of Ultralarge Reduced Graphene Oxide Monolayers. *Chem. Mater.* **2009**, *21*, 5674–5680.
36. Zhou, X. F.; Liu, Z. P. A Scalable, Solution-Phase Processing Route to Graphene Oxide and Graphene Ultra-Large Sheets. *Chem. Commun.* **2010**, *46*, 2611–2613.
37. Chen, C. M.; Yang, Q. H.; Yang, Y. G.; Lv, W.; Wen, Y. F.; Hou, P. X.; Wang, M. Z.; Cheng, H. M. Self-Assembled Free-Standing Graphite Oxide Membrane. *Adv. Mater.* **2009**, *21*, 3007–3011.
38. Pei, S. F.; Zhao, J. P.; Du, J. H.; Ren, W. C.; Cheng, H. M. Direct Reduction of Graphene Oxide Films into Highly Conductive and Flexible Graphene Films by Hydrohalic Acids. *Carbon*, published online august 8, 2010, http://dx., doi.org/10.1016/j.carbon.2010.08.006.
39. Luo, Z. T.; Lu, Y.; Somers, L. A.; Johnson, A. T. C. High Yield Preparation of Macroscopic Graphene Oxide Membranes. *J. Am. Chem. Soc.* **2009**, *131*, 898–899.
40. Tung, V. C.; Allen, M. J.; Yang, Y.; Kaner, R. B. High-Throughput Solution Processing of Large-Scale Graphene. *Nat. Nanotechnol.* **2009**, *4*, 25–29.
41. Li, D.; Muller, M. B.; Gilje, S.; Kaner, R. B.; Wallace, G. G.

Processable Aqueous Dispersions of Graphene Nanosheets. *Nat. Nanotechnol.* **2008**, *3*, 101–105.
42. Gao, L. B.; Ren, W. C.; Li, F.; Cheng, H. M. Total Color Difference for Rapid and Accurate Identification of Graphene. *ACS Nano* **2008**, *2*, 1625–1633.
43. Cai, W. W.; Piner, R. D.; Stadermann, F. J.; Park, S.; Shaibat, M. A.; Ishii, Y.; Yang, D. X.; Velamakanni, A.; An, S. J.; Stoller, M.; *et al*. Synthesis and Solid-State NMR Structural Characterization of ^{13}C-Labeled Graphite Oxide. *Science* **2008**, *321*, 1815–1817.
44. Li, J. L.; Kudin, K. N.; McAllister, M. J.; Prud'homme, R. K.; Aksay, I. A.; Car, R. Oxygen-Driven Unzipping of Graphitic Materials. *Phys. Rev. Lett.* **2006**, *96*, 176101.
45. Ajayan, P. M.; Yakobson, B. I. Materials Science—Oxygen Breaks into Carbon World. *Nature* **2006**, *441*, 818–819.
46. Wu, Z. S.; Ren, W. C; Gao, L. B.; Liu, B. L; Zhao, J. P.; Cheng, H. M. Efficient Synthesis of Graphene Nanoribbons Sonochemically Cut from Graphene Sheets. *Nano Res.* **2010**, *1*, 16–22.
47. Jung, N.; Kim, N.; Jockusch, S.; Turro, N. J.; Kim, P.; Brus, L. Charge Transfer Chemical Doping of Few Layer Graphenes: Charge Distribution and Band Gap Formation. *Nano Lett.* **2009**, *9*, 4133–4137.
48. Kyotani, M.; Matsushita, S.; Nagai, T.; Matsui, Y.; Shimomura, M.; Kaito, A.; Akagi, K. Helical Carbon and Graphitic Films Prepared from Iodine-Doped Helical Polyacetylene Film Using Morphology-Retaining Carbonization. *J. Am. Chem. Soc.* **2008**, *130*, 10880–10881.
49. De, S.; Coleman, J. N. Are There Fundamental Limitations on the Sheet Resistance and Transmittance of Thin Graphene Films. *ACS Nano* **2010**, *4*, 2713–2720.
50. Chen, C. M.; Yang, Y. G.; Wen, Y. F.; Yang, Q. H.; Wang, M. Z. Preparation of Ordered Graphene-Based Conductive Membrane. *New Carbon Mater.* **2008**, *23*, 345–350.